

SIMPLIFIED MAP DESPECKLING BASED ON LAPLACIAN-GAUSSIAN MODELING OF UNDECIMATED WAVELET COEFFICIENTS

Fabrizio Argenti, Tiziano Bianchi, Alessandro Lapini, and Luciano Alparone

Dipartimento di Elettronica e Telecomunicazioni – University of Florence

Via di Santa Marta, 3 – 50139 - Firenze - Italy

E-mail: {fabrizio.argenti,tiziano.bianchi,alessandro.lapini}@unifi.it, alparone@lci.unifi.it

ABSTRACT

The undecimated wavelet transform and the maximum a posteriori (MAP) criterion have been applied to the problem of despeckling SAR images. The solution is based on the assumption that the wavelet coefficients have a known distribution; in previous works, the generalized Gaussian function has been successfully employed. Furthermore, despeckling methods can be improved by using a classification of the wavelet coefficients according to their texture energy. A major drawback of using the generalized Gaussian distribution is the high computational cost, since the MAP solution can be found only numerically.

In this work, a new modeling of the statistics of the wavelet coefficients is proposed. The observation of the experimental estimated generalized Gaussian shape parameters related to the reflectivity and to speckle noise suggests that their distributions can be approximated as a Laplacian and as a Gaussian function, respectively. Under these hypotheses, a closed form solution of the MAP estimation problem can be achieved. As for the generalized Gaussian case, classification of the wavelet coefficients according to their texture content can also be exploited in the new proposed method. The experimental results show that the fast MAP estimator based on the Laplacian-Gaussian assumption and on coefficient classification reaches almost the same performances of the generalized Gaussian counterpart in terms of speckle removal, with a computational gain of about one order of magnitude.

1. INTRODUCTION

Speckle removal is a major problem in the analysis of SAR images. Speckle noise is a granular disturbance that affects the observed reflectivity. Usually, it is modeled as a multiplicative noise: this nonlinear behavior makes the process of original information retrieval a nontrivial task [1]-[3]. In the recent years, multiresolution analysis tools have been successfully applied [4]-[7]. Despeckling can be seen as an estimation problem. As such, the proposed statistical despeckling methods can be classified according to the estimation criterion and to the models of the processes that are involved. Bayesian methods, such as LMMSE and MAP criteria, have been taken into consideration both in the spatial and in the wavelet domain, e.g., in [1][2][5][7]. Different distributions have been considered in several works dealing with MAP estimation in the wavelet domain: the Γ -distribution [2], the α -stable distribution [4], the Pearson system of distributions

[5], the generalized Gaussian (GG) [8][9], to cite some examples.

In [8], it has been shown that the MAP criterion in the undecimated wavelet domain, associated with the GG distribution, leads to the following procedure: 1) estimation of the spatially varying parameters of the GG distribution of the wavelet coefficients associated to the speckle-free reflectivity and to the speckle noise; 2) solution of the MAP equation. The latter step is performed numerically, thus leading to a high computational cost to achieve the solution. The method in [8] has been refined in [9], where a model for the classification of the wavelet coefficients according to their texture energy was introduced. The model allowed the authors to classify the wavelet coefficients into classes having different degrees of heterogeneity, so that ad hoc estimation approaches can be devised for the different sets of coefficients. Different implementations, characterized by different approaches for incorporating into the filtering procedure the information deriving from the segmentation of the wavelet coefficients, were proposed. The experimental results in [9] demonstrated that the proposed filtering approach outperformed previously proposed filters.

One of the major drawback of GG-based MAP solutions, either with or without classification of the wavelet coefficients, is that they can be achieved only numerically. Experimental results suggest that the estimated distributions of the wavelet coefficients relative to the speckle-free reflectivity and to the speckle noise follow, approximately, a Laplacian and a Gaussian distribution, respectively. Under these assumptions, it is shown that the MAP equation can be solved in a closed form. The computational cost can be reduced of one order of magnitude or more with respect to the solution obtained numerically with the GG assumption, without significantly affecting the performance in terms of speckle reduction.

As in the case of the GG-based MAP solution, also for the Laplacian-Gaussian (LG) based method an improvement of the performances can be achieved by using a classification of the wavelet coefficients according to their texture content and by using different filtering strategies over the different classes.

2. MAP DESPECKLING IN THE UNDECIMATED WAVELET DOMAIN

In this section, some results from [8] are reviewed and the experimental observations that lead us to a new wavelet coefficients modeling are presented.

This study has been carried out under the financial support of Italian Space Agency (ASI), Cosmo-Skymed Scientific Projects, under contract I/043/09/0.

2.1 Signal model and undecimated wavelet transform

It is assumed that the observed signal follows the model

$$g[n] = f[n] \cdot u[n] = f[n] + f[n] \cdot (u[n] - 1) = f[n] + v[n], \quad (1)$$

where $g[n]$ is the observed signal; $f[n]$ is the speckle-free reflectivity we would like to estimate; $u[n]$ is the speckle noise; $v[n]$ accounts for speckle disturbance in the equivalent additive model. The speckle $u[n]$ is assumed as white and independent from $f[n]$, whereas $v[n]$ is signal-dependent. For the simplicity's sake, the model is formulated in one dimension.

Let $W_x^{[j]}$ be the undecimated wavelet operator applied to the signal x . It performs a multiresolution decomposition, where j is the level of the decomposition. Thanks to the linearity of the operator, we have

$$W_g^{[j]}[n] = W_f^{[j]}[n] + W_v^{[j]}[n]. \quad (2)$$

To simplify the notation, the level j and the index n (when not strictly necessary) are omitted in the following.

Despeckling in the multiresolution domain means estimating the speckle-free wavelet coefficients $\hat{W}_f[n]$ and applying the inverse undecimated wavelet transform.

2.2 MAP estimation

The MAP estimator of the speckle-free wavelet coefficients is given by

$$\hat{W}_f = \arg \max_{W_f} p(W_f | W_g), \quad (3)$$

or, after applying the Bayes rule and the log function, by the equation

$$\hat{W}_f = \arg \max_{W_f} [\log p(W_g | W_f) + \log p(W_f)] \quad (4)$$

2.3 Analysis of the GG Shape Parameter

In [8], a GG function is proposed to model the wavelet coefficients pdf's involved in (4). The zero-mean GG distribution is given by

$$p_{GG}(\theta) = \frac{\nu \eta}{2\Gamma(1/\nu)} e^{-(\eta|\theta|)^\nu}, \quad (5)$$

where ν is a *shape* parameter and η is a *scale* parameter, given by

$$\eta = \frac{1}{\sigma} \left[\frac{\Gamma(3/\nu)}{\Gamma(1/\nu)} \right]^{1/2}. \quad (6)$$

It is well-known that the GG distribution coincides with the Laplacian distribution for $\nu = 1$ and with the Gaussian distribution for $\nu = 2$. In [8], it is shown that the shape parameter can be estimated by solving the following equation in the unknown ν

$$\frac{E[X^2]}{\sqrt{E[X^4]}} = \frac{\Gamma(3/\nu)}{\sqrt{\Gamma(1/\nu)\Gamma(5/\nu)}}, \quad (7)$$

where $E[X^2]$ and $E[X^4]$ are the second and the fourth-order moments of the GG-distributed random variable X . In the actual implementation, such moments are "locally" evaluated from the observed signal and from the knowledge of the model (1) (see [8] for the details).

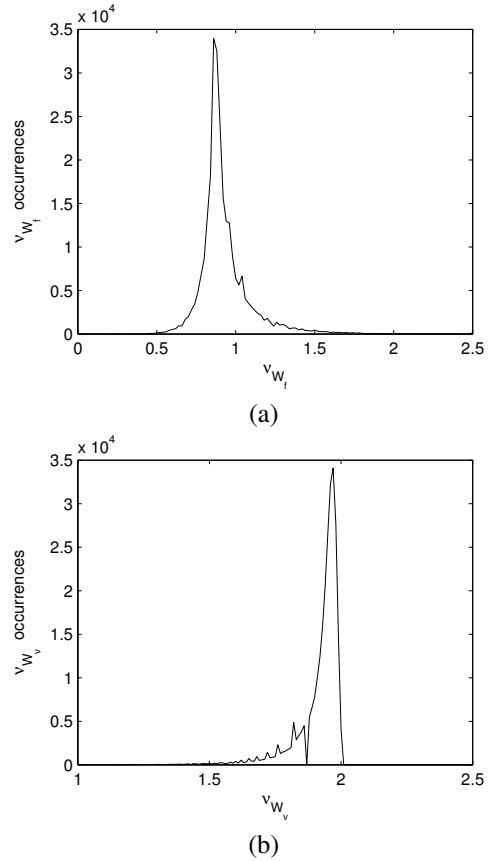


Figure 1: Examples of the histogram of the estimated shape parameters: (a) wavelet coefficients of the speckle-free signal; (b) wavelet coefficients of the signal-dependent noise.

Some experimental observations of the shape parameters suggest us that the GG assumption for the distributions of the wavelet coefficients can be simplified. As to the pdf's of the wavelet coefficients of the speckle-free signal, i.e., $p_{W_f}(W_f)$, an example of the histogram of the estimated shape parameters, obtained from the test image *Lena*, is shown in Figure 1-(a): as can be seen, in a first approximation, we may assume that they roughly approach the value 1. An analogous example, relative to the pdf's of the wavelet coefficients of the signal-dependent noise, i.e., $p(W_g | W_f) = p_{W_v}(W_g - W_f)$, is shown in Figure 1-(b): in this case, we may assume that the shape parameters approach the value 2. A behavior similar to that shown in these examples has been also encountered for different subbands and different decomposition levels.

In the remainder of this paper, we will show that if we assume that the wavelet coefficients related to the speckle-free signal and to the signal-dependent noise are distributed as a Laplacian and as a Gaussian function, respectively (*LG* assumption), then the solution of the MAP equation can be found in a closed form and, therefore, with a limited computational burden. The LG assumption has been used in other works to derive MAP and MMSE estimators [10][11]. A major difference with respect to the work presented here is that in [11] homomorphic filtering was used. Such pre-processing, however, may induce a biased estimation and we preferred to avoid it.

3. LG DESPECKLING FILTERS

3.1 LG-MAP despeckling

The proposed method is based on equation (4) that, by using a simplified notation and the model in (2), can be rewritten as

$$\hat{\theta} = \arg \max_{\theta} [\log p_v(x - \theta) + \log p_{\theta}(\theta)], \quad (8)$$

where $\theta = W_f[n]$, $x = W_g[n]$, and $v = W_v[n]$.

According to the experimental results presented in section 2.3, we will assume that the distribution of θ is a Laplacian and that of v is a Gaussian function; specifically, they are distributed as follows:

$$p_v(v) = \frac{1}{\sqrt{2\pi}\sigma_v} e^{-\frac{(v-\mu_v)^2}{2\sigma_v^2}}, \quad p_{\theta}(\theta) = \frac{1}{\sqrt{2}\sigma_{\theta}} e^{-\frac{\sqrt{2}|\theta-\mu_{\theta}|}{\sigma_{\theta}}} \quad (9)$$

In [7], it has been demonstrated that, for the noise component v , we have

$$E[v] = 0, \quad (10)$$

$$\sigma_v^2 = E[v^2] = \frac{\sigma_{u'}^2}{1 + \sigma_{u'}^2} \sum_i h^2[i] E[g^2[n-i]], \quad (11)$$

where $h[n]$ is the “equivalent” filter [7] that yields the wavelet coefficients of a given subband and $\sigma_{u'}^2$ is the variance of the variable $u' = u - 1$. For the signal component θ , instead, we have

$$E[\theta] = E[x], \quad (12)$$

$$\sigma_{\theta}^2 = \sigma_x^2 - E[v^2]. \quad (13)$$

From the above expressions, we can conclude that the moments of the variables v and θ can be written as a function of the moments of the observed signal and of the observed wavelet coefficients (these quantities are estimated as local averages).

The MAP equation can be written as

$$\begin{aligned} \hat{\theta} &= \arg \max_{\theta} \left[\log \frac{1}{\sqrt{2}\sigma_{\theta}} e^{-\frac{\sqrt{2}|\theta-\mu_{\theta}|}{\sigma_{\theta}}} + \log \frac{1}{\sqrt{2\pi}\sigma_v} e^{-\frac{(x-\theta)^2}{2\sigma_v^2}} \right] \\ &= \arg \min_{\theta} \left[\frac{\sqrt{2}|\theta-\mu_{\theta}|}{\sigma_{\theta}} + \frac{(x-\theta)^2}{2\sigma_v^2} \right]. \end{aligned} \quad (14)$$

The solution to this optimization problem is given by

$$\hat{\theta} = \begin{cases} x - \frac{\sqrt{2}\sigma_v^2}{\sigma_{\theta}} & \text{if } x > \mu_{\theta} + \frac{\sqrt{2}\sigma_v^2}{\sigma_{\theta}} \\ x + \frac{\sqrt{2}\sigma_v^2}{\sigma_{\theta}} & \text{if } x < \mu_{\theta} - \frac{\sqrt{2}\sigma_v^2}{\sigma_{\theta}} \\ \mu_{\theta} & \text{elsewhere.} \end{cases} \quad (15)$$

The proof can be easily obtained as follows. Consider, e.g., the case $\theta < \mu_{\theta}$: equation (14) becomes

$$\hat{\theta} = \arg \min_{\theta} \left[-\frac{\sqrt{2}(\theta-\mu_{\theta})}{\sigma_{\theta}} + \frac{(x-\theta)^2}{2\sigma_v^2} \right]. \quad (16)$$

Differentiating with respect to θ yields a zero for

$$\theta = x + \frac{\sqrt{2}\sigma_v^2}{\sigma_{\theta}} \quad (17)$$

Substituting this expression into the initial assumption $\theta < \mu_{\theta}$ yields $x > \mu_{\theta} - \frac{\sqrt{2}\sigma_v^2}{\sigma_{\theta}}$. The other cases can be derived in a similar way.

3.2 LG-MAP with Segmentation

In [9], it was demonstrated that the performance of the GG-MAP filter can be noticeably improved using a segmented approach, where each wavelet subband is divided into different classes of heterogeneity according to the texture energy of the wavelet coefficients of noise-free reflectivity. The key point is to assume that the wavelet coefficients within a particular class follow the same GG distribution, so that the parameters of the GG model can be accurately estimated within each class.

A similar approach can be applied in the case of the LG-MAP filter. Here, the key observation is that the LG model may be well suited only for a particular class of heterogeneity, whereas for other classes it may be better to use alternative models. According to the class each wavelet coefficient belongs to, we propose to apply the following three processing strategies.

- Wavelet coefficients belonging to the lower energy class are processed using the LG-MAP filter we propose in this paper. This class represents the set of coefficients of weakly textured areas, or homogeneous areas, which are better approximated by the assumption of Laplacian distribution.
- Wavelet coefficients belonging to the middle energy class are processed using the LMMSE filter proposed in [7]. The LMMSE filter is a general-purpose first-order approximation filter and it represents the optimal MAP filter when both the coefficients of noise-free reflectivity and the coefficients of speckle noise follow a normal distribution. We assume that this hypothesis is sufficiently valid for coefficients belonging to heterogeneous areas.
- Wavelet coefficients belonging to the last class are supposed to represent strongly heterogeneous areas or point targets. Because these areas do not follow any longer the fully-developed speckle model, the wavelet coefficients of the last class are left unchanged.

In the following, the above filtering strategy will be referred to as LG-MAP-SEG filter.

4. EXPERIMENTAL RESULTS

In this section, the experimental results obtained with the algorithms previously described are compared in terms of speckle removal efficiency and computational burden. In order to ascertain the performance loss/gain of the LG vs the GG assumption, a first set of quantitative results obtained by using a 8 bit 512×512 test image (*Lena*), degraded by synthetically generated speckle noise, are shown. Then, some results derived from a true SAR image are also presented.

In the case of synthetically generated speckle degradation, the quality of the filtered image can be measured by means of the peak SNR (PSNR), given by $PSNR = 10 \log_{10} 255^2 / MSE$, where MSE is the mean square error between the original and the filtered image.

A more general method to assess the effectiveness of the different filters, which can be used also when the noise-free reference image is not available, is based on the statistics of the ratio image, defined as $\hat{u} = g/\hat{f}$, where \hat{f} represents the estimated noise-free reflectivity. When a fully-developed speckle model can be assumed, the above image represents the filtered out speckle noise. Hence, for a good despeckling filter \hat{u} should satisfy $E[\hat{u}] = 1$ and $Var[\hat{u}] = 1/L$, where L is

Table 3: Mean and variance of extracted noise \hat{u} , measured on synthetically corrupted *Lena* through scatter-plot method.

	1-look		2-look		4-look		16-look	
	$\mu_{\hat{u}}$	$\sigma_{\hat{u}}^2$	$\mu_{\hat{u}}$	$\sigma_{\hat{u}}^2$	$\mu_{\hat{u}}$	$\sigma_{\hat{u}}^2$	$\mu_{\hat{u}}$	$\sigma_{\hat{u}}^2$
LMMSE	0.9278	0.6978	0.9568	0.3602	0.9752	0.1863	0.9919	0.0465
GG-MAP-SEG	0.9854	0.9359	0.9883	0.4755	0.9919	0.2385	0.9966	0.0597
LG-MAP	0.9787	0.8974	0.9849	0.4553	0.9892	0.2304	0.9941	0.0576
LG-MAP-SEG	0.9787	0.8974	0.9848	0.4553	0.9891	0.2303	0.9945	0.0573

Table 1: PSNR obtained by using *Lena* degraded by synthetically generated speckle.

	1-look	2-look	4-look	16-look
LMMSE	24.59	26.62	28.57	32.61
GG-MAP-SEG	26.40	28.04	29.77	33.24
LG-MAP	26.21	27.77	29.41	32.95
LG-MAP-SEG	26.21	27.82	29.55	33.27

Table 2: Order of magnitude of the computational times (in seconds) of the analyzed algorithms for 512×512 images.

	computational cost (s)
LMMSE	10^1
GG-MAP-SEG	10^2
LG-MAP	10^1
LG-MAP-SEG	10^1

the number of look [3].

The mean and the variance of the ratio image are estimated by using a scatter plot method similar to that proposed in [12]. The method consists of the following steps. First, a scatter plot is obtained by plotting the occurrences of each pair of local mean and standard deviation, calculated on a moving local window over the image \hat{u} . Hence, the bivariate probability density function (pdf) is estimated from the scatter plot, and the mean and standard deviation of \hat{u} are estimated as the coordinates of the maximum of the bivariate pdf. The rationale of this method is based on the assumption that each local window would give a contribution centered on such a maximum if the size of the window is sufficiently large. Thanks to using statistics computed on local windows, the above method is accurate also in the case of real SAR images, for which the assumption of fully-developed speckle is not valid everywhere and global statistics would be biased due to the presence of outliers.

The despeckling filters that are compared in the following are: the LMMSE filter presented in [7]; the GG-MAP-SEG filter proposed in [9]; the LG-MAP filter proposed in section 3.1; the LG-MAP-SEG filter proposed in section 3.2.

In Table 1, the performance of the despeckling filters are compared in terms of PSNR. The order of magnitude of the computational times, expressed in seconds and related to our Matlab implementation, are shown in Table 2. As can be seen, the complexity of the LG filters is the same as the LMMSE one. However, especially for multilook images, the performance of the LG-MAP-SEG filter is very close to that of the GG-MAP-SEG filter, showing that a valuable com-

Table 4: Mean and variance of extracted noise \hat{u} , measured on nominal 4-look SAR image *Airport* through scatter-plot method.

	$\mu_{\hat{u}}$	$\sigma_{\hat{u}}^2$
LMMSE	0.9298	0.1584
GG-MAP-SEG	0.9722	0.2878
LG-MAP	0.9606	0.2540
LG-MAP-SEG	0.9583	0.2515

putational gain is achieved at the price of almost unaltered performances in terms of PSNR. These results are confirmed by the observation of Table 3, where the mean and the variance of \hat{u} , estimated by using the scatter plot method on the test image *Lena* for the different algorithms, are shown.

As to the results on true SAR data, they have assessed by using a 8 bit 512×512 X-HH 4-look image representing an airport in Ontario. The original image, is shown in Figure 2; the despeckled versions obtained with the LMMSE, GG-MAP-SEG, LG-MAP, and LG-MAP-SEG filters are also shown in Figure 2. In Table 4, the mean and the variance of \hat{u} , estimated by using the scatter plot method on the airport image for the different methods, are shown. From Table 4, we observe that the LG methods have similar performances as the GG-MAP-SEG method and outperform the LMMSE one. It can be also observed that the performances of the LG-MAP and the LG-MAP-SEG are almost identical, highlighting that they behave in the same way in fully developed speckle areas. However, comparing Figures 2-(d) and 2-(e), we observe that the LG-MAP-SEG yields a better preservation of texture details.

5. CONCLUSIONS

The MAP estimator, operating in the undecimated wavelet domain, with coefficients of reflectivity and noise both modeled as generalized Gaussian densities, has been demonstrated to be successful for removing speckle noise in SAR images. However, only a numerical solution, affected by a high computational burden, has been achieved. In this paper, based on the observation of the experimental histograms of the shape factors, the assumption of Laplacian reflectivity and Gaussian noise is made and a closed form solution is found. The Laplacian-Gaussian modeling is also combined with a segmentation-based approach, in which different filtering strategies are applied according to the heterogeneity of wavelet coefficients. The experimental results show that the performance of the fast algorithms, assessed on both simulated speckled images and on a true high-resolution X-HH 4-look image, are comparable with those of the GG-based so-

lutions, with a computational complexity more than ten times lower.

REFERENCES

- [1] D. T. Kuan, A. A. Sawchuck, T. C. Strand, and P. Chavel, "Adaptive noise smoothing filter for images with signal-dependent noise," *IEEE Trans. on Pattern Anal. and Mach. Intell.*, vol. PAMI-7, no. 2, pp. 165–177, Feb. 1985.
- [2] A. Lopes, R. Touzi, and E. Nezry, "Structure detection and statistical adaptive speckle filtering in SAR images," *International Journal of Remote Sensing*, vol. 14, no. 9, pp. 1735–1758, 1993.
- [3] R. Touzi, "A Review of Speckle Filtering in the Context of Estimation Theory," *IEEE Trans. on Geosci. and Remote Sens.*, vol. 40, no. 11, pp. 2392–2404, Nov. 2002.
- [4] A. Achim, P. Tsakalides, and A. Bezerianos, "SAR image denoising via Bayesian wavelet shrinkage based on heavy-tailed modeling," *IEEE Trans. on Geosci. and Remote Sens.*, vol. 41, no. 8, pp. 1773–1784, Aug. 2003.
- [5] S. Foucher, G. B. Bénéic, and J.-M. Boucher, "Multi-scale MAP filtering of SAR images," *IEEE Trans. on Image Proc.*, vol. 10, no. 1, pp. 1019–1036, Jan. 2001.
- [6] S. Solbø and T. Eltoft, "T-WMAP: a statistical speckle filter operating in the wavelet domain," *International Journal of Remote Sensing*, vol. 25, no. 5, pp. 1019–1036, Mar. 2004.
- [7] F. Argenti and L. Alparone, "Speckle removal from SAR images in the undecimated wavelet domain," *IEEE Trans. on Geosci. and Remote Sens.*, vol. 40, no. 11, pp. 2363–2374, Nov. 2002.
- [8] F. Argenti, T. Bianchi, and L. Alparone, "Multiresolution MAP despeckling of SAR images based on locally adaptive generalized Gaussian pdf modeling," *IEEE Trans. on Image Proc.*, vol. 15, no. 11, pp. 3385–3399, Nov. 2006.
- [9] T. Bianchi, F. Argenti, and L. Alparone, "Segmentation-based MAP despeckling of SAR images in the undecimated wavelet domain," *IEEE Trans. on Geosci. and Remote Sens.*, vol. 46, no. 9, pp. 2728–2742, Sept. 2008.
- [10] S. Gazor and Wei Zhang, "Speech enhancement employing Laplacian-Gaussian mixture," *IEEE Trans. on Speech and Audio Processing*, vol. 13, no. 5, pp. 896–904, Sept. 2005.
- [11] H. Rabbani, M. Vafadust, P. Abolmaesumi, and S. Gazor, "Speckle noise reduction of medical ultrasound images in complex wavelet domain using mixture priors," *IEEE Trans. on Biomedical Engineering*, vol. 55, no. 9, pp. 2152–2160, Sept. 2008.
- [12] B. Aiazzi, L. Alparone, S. Baronti, and A. Garzelli, "Coherence estimation from incoherent multilook SAR imagery," *IEEE Trans. Geosci. Remote Sensing*, vol. 41, no. 11, pp. 2531–2539, Nov. 2003.

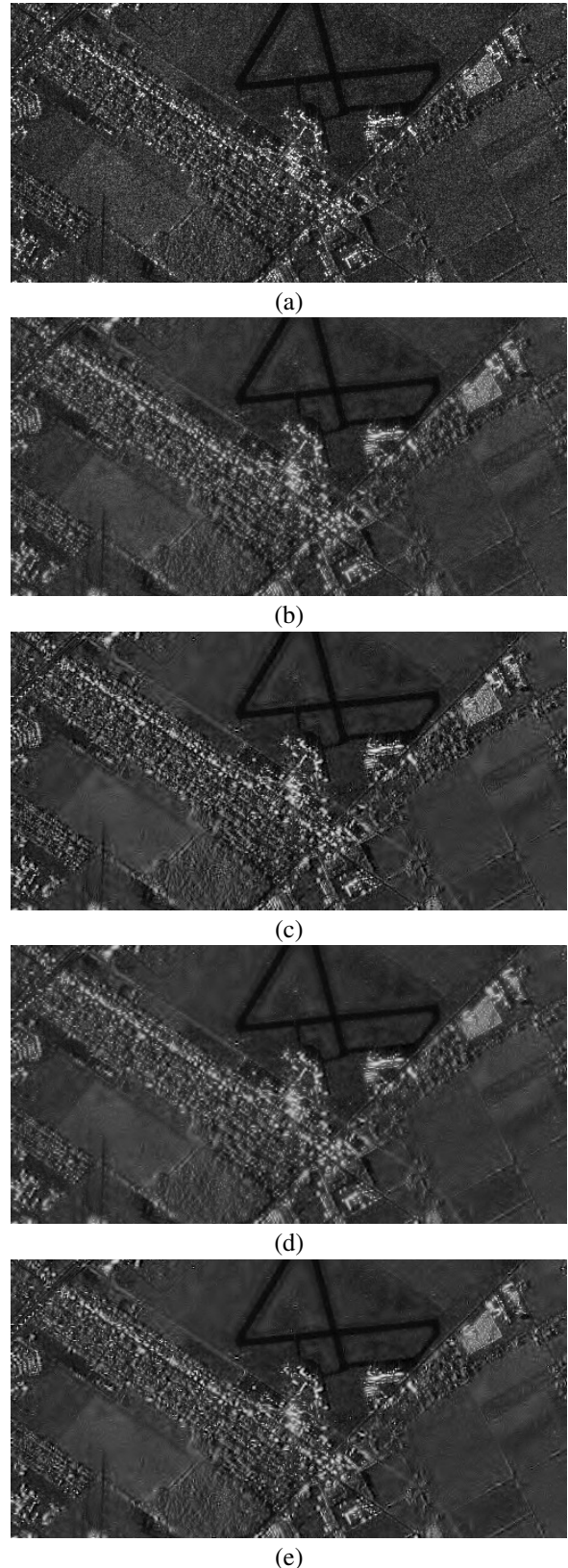


Figure 2: Results obtained by filtering nominal 4-look SAR image *Airport*, shown in (a), by using the LMMSE (b), the GG-MAP-SEG (c), the LG-MAP (d) and the LG-MAP-SEG (e) filters.